*Pramana – J. Phys.* (2017) 88: 52
DOI 10.1007/s12043-016-1354-z



# Physical hydrodynamic propulsion model study on creeping viscous flow through a ciliated porous tube

NOREEN SHER AKBAR[1], ADIL WAHID BUTT[2,*], DHARMENDRA TRIPATHI[3] and O ANWAR BÉG[4]

[1]DBS&H, CEME, National University of Sciences and Technology, Islamabad, Pakistan
[2]DBS&H, MCE, National University of Sciences and Technology, Islamabad, Pakistan
[3]Department of Mechanical Engineering, Manipal University, Jaipur 303 007, India
[4]GORT – Aerospace, Marine and Medical Engineering Sciences, Gabriel's Wing House, 11 Rooley Croft, Bradford, BD61FA, England, UK
*Corresponding author. E-mail: adil.maths86@gmail.com

MS received 7 February 2016; revised 20 July 2016; accepted 5 October 2016; published online 16 February 2017

**Abstract.** The present investigation focusses on a mathematical study of creeping viscous flow induced by metachronal wave propagation in a horizontal ciliated tube containing porous media. Creeping flow limitations are imposed, i.e. inertial forces are small compared to viscous forces and therefore a very low Reynolds number ($Re \ll 1$) is taken into account. The wavelength of metachronal wave is also considered to be very large for cilia movement. The physical problem is linearized and exact solutions are developed for the differential equation problem. Mathematica software is used to compute and illustrate numerical results. The influence of slip parameter and Darcy number on velocity profile, pressure gradient and trapping of bolus are discussed with the aid of graphs. It is found that with increasing magnitude of the slip parameter, the trapped bolus inside the streamlines increases in size. The study is relevant to biological propulsion of medical micromachines in drug delivery.

**Keywords.** Viscous fluid; ciliated tube; porous medium; Darcy number; permeability; low Reynolds number; hydrodynamic slip; biomimetic propulsion.

**PACS No. 47.10.A**

## 1. Introduction

Biological propulsion is increasingly attracting the interest of engineers owing to its diverse applications in medicine, aerospace, naval and even geological systems. Many mathematical models have been proposed for different organisms and micro-organisms at different length scales and Reynolds numbers. The most lucid review of the subject has been given by Wu [1] in which 18 orders of magnitude have been studied for the flows ranging from microscopic organisms to large marine mammals (e.g. the blue whale). At the microscopic scale, particularly in the context of embryological systems, cilia and flagellar propulsion are of great interest. This area of biological hydrodynamic propulsion has also motivated significant interest for many decades, as elaborated by Wu [2]. Length of cilia and flagella may span from a few microns to more than 2 mm in the case of sperm flagella of some insects. Hence, cilia and flagella essentially have no difference, although they have been ascribed different terminologies prior to a proper biological examination of their structures. Cilia have been established as beating with a whip-like asymmetric mechanism which comprises both an effective stroke and a recovery stroke. Moreover, when many cilia function collectively, fluid dynamic interactions may induce beating out-of-phase, and this manifests in the generation of metachronal waves, and exacerbated hydrodynamics flow. The specific metachrony is termed symplectic (or antiplectic) when the metachronal wave is in the same (or opposite) direction as the effective stroke. These features have recently attracted attention in biomimetics and bio-inspired engineering systems, notably in medical microswimmers which offer tremendous potential in nanomedicine, drug-delivery and so forth,

as described by Feng and Cho [3]. Commonly, cells have one or two long flagella. Conversely, ciliated cells have many short cilia. For instance, the mammalian spermatozoa has a single flagellum, the unicellular green alga *Chlamydomonas* has two flagella, and the unicellular protozoan *Paramecium* is covered with a few thousand cilia. These are used for both locomotion and nutrition. In mammals, many epithelial cells are ciliated in order to sweep materials across the tissue surface. For instance, considerable numbers of cilia (more than $10^7/\text{mm}^2$) cover the surfaces of mammalian respiratory passages (the nose, pharynx, and trachea). Here they dislodge and expel particulate matter that collects in the mucus secretions of these tissues. The motion of cilia and flagella is controlled by the Stokes equations (linear) with no-slip boundary conditions on their surfaces and vanishing fluid disturbance at infinity [4]. The structure of cilia, factors which affect cilia activities, movement of cilia and flagella and the coordination of the beating of cilia have been addressed analytically by Sleigh [5]. Lardner and Shack [6] examined effects of cilia on transport flow rates in the ductus efferentes of the male reproductive tract. A mathematical model to represent the microstructure of ciliated organisms was developed by Blake [7]. In continuation of the studies on cilia movement and its importance in various fields of research, Wu [8] theoretically investigated the fluid mechanism of cilia motion. Brennen [9] presented an oscillatory thin shear layer (boundary layer) theory for cilia movement. Sleigh and Aiello [10] studied water movement by cilia. Agarwal and Uddin [11] investigated the fluid flow with variable viscosity by cilia transport; Blake [12] developed a spherical envelope approach for cilia movement. Miller [13] focussed on the movement of Newtonian fluids sustained by mechanical cilia oscillation; Barton and Raynor [14] presented an analytical approach for cilia-induced mucous flow; Smith *et al* [15] addressed effects of viscoelastic fluid flow on cilia transport. Dauptain *et al* [16] studied computationally the hydrodynamics of cilia movement from a fluid-structure interaction (FSI) viewp oint, specifically simulating *ctenophore Pleurobrachia pileus* marine micro-organisms (quasispherical geometry) for multiple flexible cilia with three-dimensional models. Khaderi and Onck [17] presented three-dimensional computations for cilia movement. Khaderi *et al* [18] further studied the non-reciprocal motion due to the beating of artificial cilia. Another interesting communication by Khaderi *et al* [19] reports on magnetically-actuated artificial cilia for microfluidic propulsion.

The above biological propulsion simulations were restricted to purely fluid media. In recent years, transport phenomena in biological porous media have also attracted significant attention. Many organs in the human body, including kidneys, lungs, tissues and the skin comprise permeable materials [20]. Porous media hydrodynamics further arises in the circulation of cerebrospinal fluid in the brain. In biomedical engineering, flow in porous media is integral to the fabrication of artificial physiological organs including artificial kidneys, gastric tract and lungs [21]. Almost invariably, biological materials (tissues etc.) are heterogeneous and exhibit anisotropy strongly. These complex constitutive properties originate from the cellular microstructure. Although intrinsically the porous media arising in different organs of the body are anisotropic, approximations can be made to simulate transport through them. A popular approach is the Darcy model which has been used for microvasculature via networks of one-dimensional segments, whereas the capillary bed is often approximated as a spatially-averaged Darcy compartment. Darcy's law and its modification assume that the rate at which a fluid flows through a permeable substance per unit area is equal to the product of the permeability (the ability of a porous material to allow a fluid to pass through it) and the pressure drop per unit length of flow, divided by the viscosity of the fluid. A porous medium is generally defined in continuum mechanics [22] as a medium which contains a number of small holes distributed throughout the matter. Khaled and Vafai [23] have shown that convective flow models for porous media are accurate for modelling hemodynamics in tumours and muscles and in particular mimick quite well the impeded transport of physiological fluids in vessels clogged with fatty cholesterol plaques and clots. Interstitial fluid mechanics also lends itself well to porous media transport because the tissue may be approximated as a medium of dispersed cells separated by connective voids, the latter permitting percolation of nutrients, minerals and other substances to cells within the tissue. Darcy's law however neglects the friction within the fluid and exchange of momentum between the fluid and the solid phases. Modifications of Darcy models have therefore been done for some time. A good example of flow with boundary condition at the interfaces of a porous medium was presented by Saffman [24]. Most physiological vessels feature porous media characteristics and considering this fact many works have been reported in literature. An interesting transport problem in porous media (of the moving boundary type) is peristalsis, and arises in intestinal fluid dynamics. Representative

studies in this area have been communicated by, for example, Miyamoto *et al* [25] who studied the two-dimensional laminar flow in a circular porous tube and considering a small water absorption or secretion in the intestinal perfusion experiment whereas Jeffrey *et al* [26] discussed the flow fields generated by peristaltic reflex in isolated guinea pig ileum. Elshehawey *et al* [27] developed another model for peristaltic transport through an asymmetric porous medium channel and focussed the application to intrauterine fluid motion in a sagittal cross-section of the uterus. Other recent investigations on peristaltic flow of Newtonian and non-Newtonian fluids spanning many multiphysical aspects of the subject include power law fluids [28], magnetohydrodynamics [29] and Maxwell rheological pumping through porous media [30].

A careful inspection of the scientific literature has revealed however that the creeping flow induced by metachronal wave propagations of viscous fluid in a porous ciliated tube is yet to be studied mathematically in the literature. Porous media offer a well-tested mechanism for flow control in hydrodynamic propulsion. The present work aims to therefore address this topic for the first time. Analytical solutions are developed for the linear partial differential equations generated. Linearization is achieved by neglecting inertial forces relative to viscous forces, using the low Reynolds number approximation from hydrodynamic lubrication theory. Numerical results are presented graphically and the influence of key geometric and hydromechanical parameters (e.g. Darcy number) on transport characteristics is elaborated in detail. The simulations presented herein further elucidate the mechanism of creeping viscous flow induced by cilia motion and are relevant to gastric fluid mechanics and also biomimetic devices exploiting surface modifications for optimized propulsion [31–35].

## 2. Mathematical model

Let us consider incompressible Newtonian flow in a ciliated tube with hydrodynamic slip at the wall. The interior wall of the tube is ciliated with metachronal waves and the flow is generated due to the collective beating of cilia. We select a cylindrical coordinate system $(\bar{R}, \bar{Z})$, where the $\bar{Z}$-axis is orientated alongthe centre line of the tube and $\bar{R}$-axis is normal to it. Cilia deform in a wave-like fashion with a propagation velocity, $c$, along the wall of the outer tube. Keeping in view the geometry of the metachronal wave pattern, it is assumed that the envelope of cilia tips can be expressed mathematically in the following form [1,9] (figure 1):

$$\bar{R} = \bar{H} = \bar{f}(\bar{Z}, \bar{t}) = a + a\varepsilon \cos\left(\frac{2\pi}{\lambda}(\bar{Z} - c\bar{t})\right),$$

$$\bar{Z} = \bar{g}(\bar{Z}, \bar{Z}_0, \bar{t}) = a + a\varepsilon\alpha \sin\left(\frac{2\pi}{\lambda}(\bar{Z} - c\bar{t})\right), \quad (1)$$

where $a$ denotes the mean radius of the tube, $\varepsilon$ is the non-dimensional measure with respect to the cilia length, $\lambda$ and $c$ are the wavelength and speed of the metachronal wave respectively, $\bar{Z}_0$ denotes the reference position of the particle and $\alpha$ is a measure of the eccentricity of the elliptical motion. The velocities of the transport fluid are essentially those induced by the cilia tips, and may be defined as

$$\bar{W} = \left(\frac{\partial \bar{Z}}{\partial \bar{t}}\right)_{\bar{Z}_0} = \frac{\partial \bar{g}}{\partial \bar{t}} + \frac{\partial \bar{g}}{\partial \bar{Z}}\frac{\partial \bar{Z}}{\partial \bar{t}} = \frac{\partial \bar{g}}{\partial \bar{t}} + \frac{\partial \bar{g}}{\partial \bar{Z}}\bar{W},$$

$$\bar{U} = \left(\frac{\partial \bar{R}}{\partial \bar{t}}\right)_{\bar{Z}_0} = \frac{\partial \bar{f}}{\partial \bar{t}} + \frac{\partial \bar{f}}{\partial \bar{Z}}\frac{\partial \bar{Z}}{\partial \bar{t}} = \frac{\partial \bar{f}}{\partial \bar{t}} + \frac{\partial \bar{f}}{\partial \bar{Z}}\bar{W}. \quad (2)$$

Using eq. (2) in (1), we get

$$\bar{W} = \frac{-(2\pi/\lambda)[\varepsilon\alpha ac \cos(2\pi/\lambda)(\bar{Z} - c\bar{t})]}{[1 - (2\pi/\lambda)\{\varepsilon\alpha a \cos(2\pi/\lambda)(\bar{Z} - c\bar{t})\}]},$$

$$\bar{U} = \frac{(2\pi/\lambda)[\varepsilon ac \sin(2\pi/\lambda)(\bar{Z} - c\bar{t})]}{[1 - (2\pi/\lambda)\{\varepsilon\alpha a \cos(2\pi/\lambda)(\bar{Z} - c\bar{t})\}]}. \quad (3)$$

In the fixed coordinates $(\bar{R}, \bar{Z})$, the flow in the tube is unsteady. It becomes steady in a wave frame $(\bar{r}, \bar{z})$ moving with the same speed as the wave moves in the $\bar{Z}$-direction. The governing equations for the viscousflow through porous medium in the moving frame is expressed as

*Continuity equation*:

$$\frac{1}{\bar{R}}\frac{\partial(\bar{R}\bar{U})}{\partial \bar{R}} + \frac{\partial \bar{W}}{\partial \bar{Z}} = 0. \quad (4)$$

*R-direction momentum equation*:

$$\rho\left[\frac{\partial\bar{U}}{\partial\bar{t}}+\bar{U}\frac{\partial\bar{U}}{\partial\bar{R}}+\bar{W}\frac{\partial\bar{U}}{\partial\bar{Z}}\right]=-\frac{\partial\bar{P}}{\partial\bar{R}}+\mu\frac{\partial}{\partial\bar{R}}\left[2\frac{\partial\bar{U}}{\partial\bar{R}}\right]+\mu\frac{2}{\bar{R}}\left(\frac{\partial\bar{U}}{\partial\bar{R}}-\frac{\bar{U}}{\bar{R}}\right)+\mu\frac{\partial}{\partial\bar{Z}}\left[\left(\frac{\partial\bar{U}}{\partial\bar{R}}+\frac{\partial\bar{W}}{\partial\bar{Z}}\right)\right]. \quad (5)$$

*Z-direction momentum equation*:

$$\rho\left[\frac{\partial\bar{W}}{\partial\bar{t}}+\bar{U}\frac{\partial\bar{W}}{\partial\bar{R}}+\bar{W}\frac{\partial\bar{W}}{\partial\bar{Z}}\right]=-\frac{\partial\bar{P}}{\partial\bar{Z}}+\mu\frac{\partial}{\partial\bar{Z}}\left[2\frac{\partial\bar{W}}{\partial\bar{Z}}\right]+\mu\frac{1}{\bar{R}}\frac{\partial}{\partial\bar{R}}\left[\bar{R}\left(\frac{\partial\bar{U}}{\partial\bar{Z}}+\frac{\partial\bar{W}}{\partial\bar{R}}\right)\right]-\frac{\mu}{K}\bar{W}. \quad (6)$$

The transformations between the two frames are:

$$\bar{r}=\bar{R},\quad \bar{z}=\bar{Z}-c\bar{t},\quad \bar{u}=\bar{U},$$
$$\bar{w}=\bar{W}-c,\quad \bar{p}(\bar{z},\bar{r})=\bar{P}(\bar{Z},\bar{R},\bar{t}). \quad (7)$$

The governing equations for the regime can be written via these transformations as follows:

$$\frac{1}{\bar{r}}\frac{\partial(\bar{r}\bar{u})}{\partial\bar{r}}+\frac{\partial\bar{w}}{\partial\bar{z}}=0, \quad (8)$$

$$\rho\left[\bar{u}\frac{\partial\bar{u}}{\partial\bar{r}}+\bar{w}\frac{\partial\bar{u}}{\partial\bar{r}}\right]=-\frac{\partial\bar{P}}{\partial\bar{r}}+\mu\frac{\partial}{\partial\bar{r}}\left[2\frac{\partial\bar{u}}{\partial\bar{r}}\right]+\mu\frac{2}{\bar{r}}\left(\frac{\partial\bar{u}}{\partial\bar{r}}-\frac{\bar{u}}{\bar{r}}\right)+\mu\frac{\partial}{\partial\bar{z}}\left[\left(\frac{\partial\bar{u}}{\partial\bar{r}}+\frac{\partial\bar{w}}{\partial\bar{z}}\right)\right], \quad (9)$$

$$\rho\left[\bar{u}\frac{\partial\bar{w}}{\partial\bar{r}}+\bar{w}\frac{\partial\bar{w}}{\partial\bar{z}}\right]=-\frac{\partial\bar{P}}{\partial\bar{z}}+\mu\frac{\partial}{\partial\bar{z}}\left[2\frac{\partial\bar{w}}{\partial\bar{z}}\right]+\mu\frac{1}{\bar{r}}\frac{\partial}{\partial\bar{r}}\left[\bar{r}\left(\frac{\partial\bar{u}}{\partial\bar{z}}+\frac{\partial\bar{w}}{\partial\bar{r}}\right)\right]-\frac{\mu}{K}(\bar{w}+c), \quad (10)$$

Corresponding boundary conditions are as defined in Ellahi *et al* [31], Nadeem and Sadaf [35].

$$\frac{\partial\bar{w}}{\partial\bar{r}}=0,\quad \text{at } r=0,$$
$$w=-1-\frac{2\pi\varepsilon\alpha\beta\cos(2\pi z)}{1-2\pi\varepsilon\alpha\beta\cos(2\pi z)}-\frac{K}{\alpha_1^*}\frac{\partial\bar{w}}{\partial\bar{r}},\ \text{at } r=\bar{h}(z). \quad (11)$$

where $2\pi\varepsilon\alpha\beta\cos(2\pi z)/[1-2\pi\varepsilon\alpha\beta\cos(2\pi z)]$ is the cilia factor.

Introducing the following non-dimensional variables

$$r=\frac{\bar{r}}{a},\quad z=\frac{\bar{z}}{\lambda},\quad w=\frac{\bar{w}}{c},\quad u=\frac{\lambda\bar{u}}{ac},\quad p=\frac{a^2\bar{p}}{c\lambda\mu},$$
$$\beta=\frac{a}{\lambda},\quad D_a=\frac{K}{a^2},\quad \alpha_1=\frac{\alpha_1^*}{a}, \quad (12)$$

making use of these variables in eqs (9) and (10), and using the assumptions of low Reynolds number and long wavelength, the non-dimensional governing equations can be written as

$$\frac{\partial p}{\partial r}=0, \quad (13)$$

$$\frac{\mathrm{d}p}{\mathrm{d}z}=\frac{1}{r}\frac{\partial}{\partial r}\left(r\frac{\partial w}{\partial r}\right)-\frac{1}{D_a}(w+1). \quad (14)$$

The non-dimensional boundary conditions on the ciliated porous walls are prescribed as

$$\frac{\partial w}{\partial r}=0,\quad \text{at } r=0, \quad (14a)$$

$$w=-1-\frac{2\pi\varepsilon\alpha\beta\cos(2\pi z)}{1-2\pi\varepsilon\alpha\beta\cos(2\pi z)}-\frac{\sqrt{D_a}}{\alpha_1}\frac{\partial w}{\partial r},$$
$$\text{at } r=h(z)=1+\varepsilon\cos(2\pi z). \quad (14b)$$

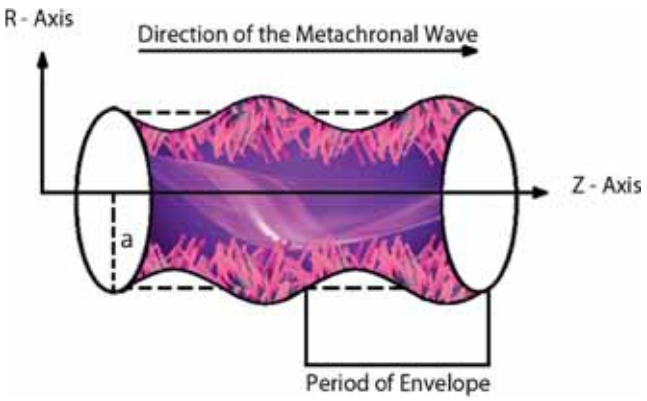


**Figure 1.** Schematic of the biological propulsion problem.

## 3. Analytical solution

Integrating eq. (13) and using boundary conditions (14a, b), axial velocity is obtained as

$$w(r,\ z) = -1 - D_a \frac{\mathrm{d}p}{\mathrm{d}z} + \frac{\alpha_1 (D_a(\mathrm{d}p/\mathrm{d}z) - 2\pi\varepsilon\alpha\beta\cos(2\pi z)/(1 - 2\pi\varepsilon\alpha\beta\cos(2\pi z)))\, I_0(r/\sqrt{D_a})}{I_1(h/\sqrt{D_a}) - I_0(h/\sqrt{D_a})}. \tag{15}$$

The volumetric flow rate ($F$) is defined as

$$F = 2\pi \int_0^h r w \mathrm{d}r. \tag{16}$$

Integrating the above expression for the flow rate, we have

$$\frac{\mathrm{d}p}{\mathrm{d}z} = \frac{\dfrac{I_1\left(h/\sqrt{D_a}\right)\left((2\pi\varepsilon\alpha\beta\cos(2\pi z) - 1)(F + \pi h^2) - 2\pi\alpha_1\sqrt{D_a}hn\right)}{2\pi\varepsilon\alpha\beta\cos(2\pi z) - 1} - (F + \pi h^2)\, I_0\left(\frac{h}{\sqrt{D_a}}\right)}{\pi D_a h\left(h I_0\left(\frac{h}{\sqrt{D_a}}\right) - (h - 2\alpha_1\sqrt{D_a})\, I_1\left(\frac{h}{\sqrt{D_a}}\right)\right)}. \tag{17}$$

Flow rate in moving and fixed frames are related as follows:

$$Q = F + \frac{1}{2}\left(1 + \frac{\varepsilon^2}{2}\right). \tag{18}$$

The pressure rise ($\Delta P$) is readily found by integrating the pressure gradient with respect to $z$ over the interval [0, 1] as follows:

$$\Delta P = \int_0^1 \frac{\mathrm{d}p}{\mathrm{d}z} \mathrm{d}z. \tag{19}$$

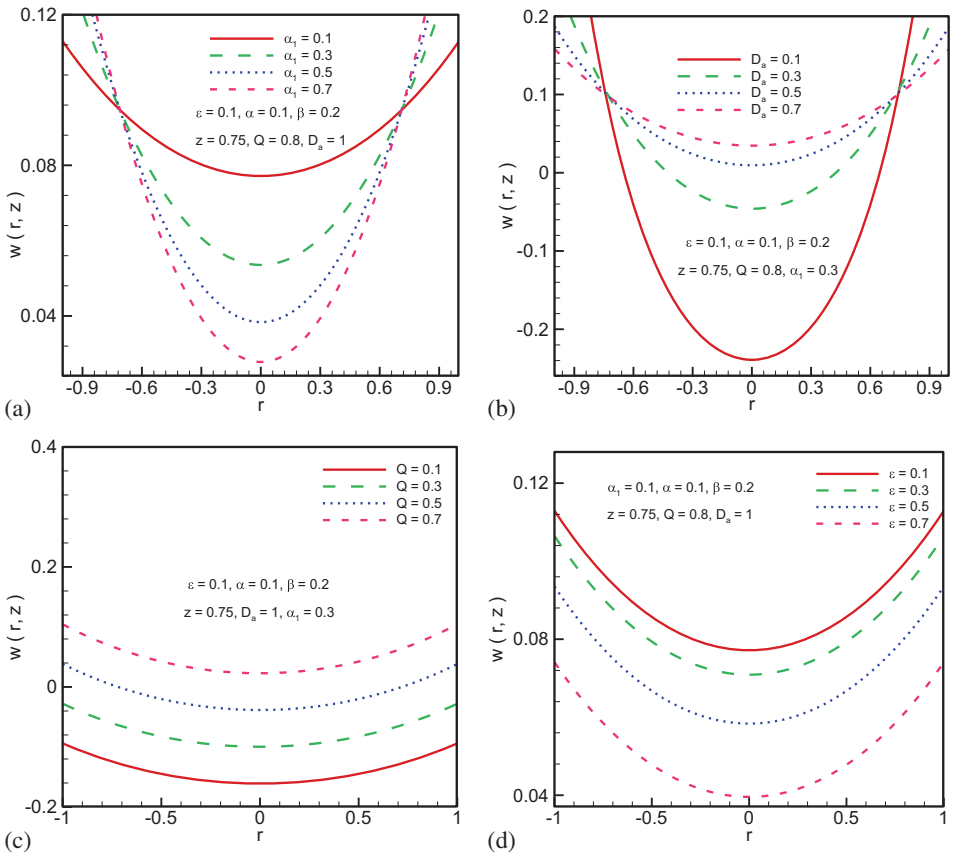


**Figure 2.** Velocity profile (axial velocity vs. radial coordinate) for (**a**) slip parameter $\alpha_1$, (**b**) Darcy number $D_a$, (**c**) flow rate $Q$ and (**d**) cilia length $\varepsilon$.

The stream function in the wave frame (obeying the Cauchy–Riemann equations, $u = \partial\psi/\partial y$ and $v = -\partial\psi/\partial x$) may be computed by using eq. (18). Visualization of streamlines is achieved with Mathematica symbolic software.

## 4. Numerical results and discussion

In this section, the effect of several physical parameters, i.e. slip parameter ($\alpha_1$) and Darcy number ($D_a$) on velocity profile, flow rate, pressure gradient and stream lines are elaborated with the help of figures 2–5.

Figures 2a–2d represent the change in the velocity of the fluid with respect to certain changes in the constraints.

The parabolic nature of the velocity profile is clearly evident from these figures. Figure 2a shows that velocity is inversely proportional to slip parameter ($\alpha_1$). Greater slip at the wall is found to counteract the development of axial momentum and manifests in a drop in axial velocity. Figure 2b depicts the effects of Darcy number on the velocity profile and it is observed that the velocity is directly proportional to the permeability of the medium. Greater permeability corresponds to a significant decrease in Darcian impedance, i.e. the drag force associated with solid fibres in the regime. Figure 2c represents the influence of flow rate on the velocity profile and it is apparent that if flow rate increases, velocity also increases. Propulsion is therefore enhanced with greater flow rates. Figure 2d reveals that velocity profile diminishes with increasing cilia length parameter ($\varepsilon$). Cilia spacing and length influence the viscous resistance per cilium and thereby the axial flow. The latter is assisted with greater cilia length and this aids in rise in pressure in the lower channel half-space. The introduction of extra energy to the flow at the lower wall however must be compensated for by an extraction at the upper wall, and these features are also related to the synchronicity of the beating cilia. The special case of $\varepsilon = 0$ implies vanishing cilia and absence of a metachronal wave – in this scenario the flow is purely peristaltic due to flexibility of the walls, and is therefore not considered here.

Figures 3a–3c illustrate the pressure rise evolution with flow rate for various parameters. A linear relation between the flow rate and pressure is observed and

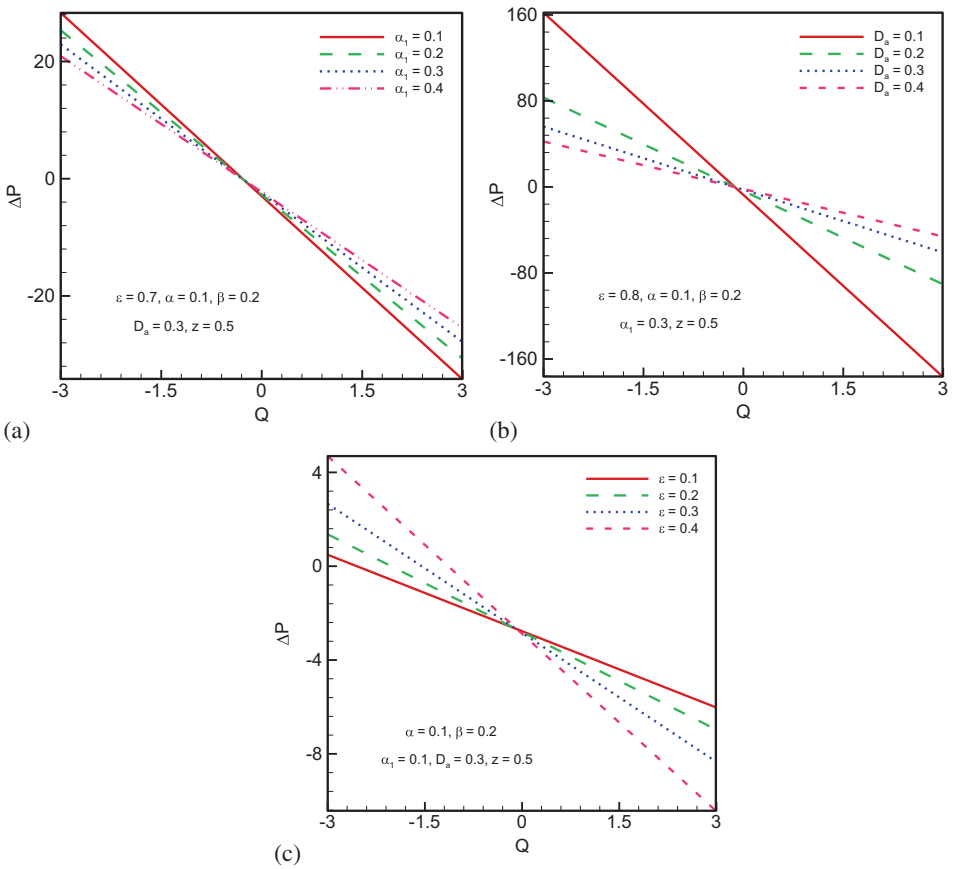


**Figure 3.** Pressure rise vs. flow rate for (**a**) slip parameter $\alpha_1$, (**b**) Darcy number $D_a$ and (**c**) cilia length $\varepsilon$.

there are three regions of pumping: (i) pumping region ($\Delta P > 0$), (ii) free pumping region ($\Delta P = 0$) and (iii) augmented pumping region ($\Delta P < 0$). The effect of slip parameter on increase in pressure is shown in figure 3a and it is evident that pressure diminishes with increase in slip parameter in the pumping region whereas the reverse response is computed in the augmented pumping region. The impact of Darcy number on pressure rise is illustrated in figure 3b and exerts a similar effect as with the slip parameter. From figure 3c, it is seen that rise in pressure is an increasing function of amplitude in the pumping region whereas it is a decreasing function in augmented pumping region.

Figures 4a–4c depict the pressure gradient distributions with axial coordinate for various hydromechanical and geometric parameters. Inspection of the figures reveals that pressure gradient increases with small changes in slip parameter and Darcy number ($\alpha_1$, $D_a$) and also cilia length ($\varepsilon$). In all cases, the maxima (peaks) exist at $z = 0.5, 1.5$. However, the relative minima varies with modification in parameter values.

Figures 5a–5d present the visualization of the streamlines under the influence of slip parameter. These streamlines constitute a family of curves which are tangential to the velocity vector at any instant of the flow. These show the direction of the fluid element at any point in time. The plots generally demonstrate that by increasing the slip parameter ($\alpha_1$), the trapped bolus inside the streamlines increases in size whereas the number of bolus decreases. In a digestive tract such as the human gastrointestinal tract, smooth muscle tissues contract in sequence to produce a peristaltic wave, which propels a ball of food (called a bolus, while in the esophagus and upper gastrointestinal tract, and chyme in the stomach). So trapped boluses are enclosed streamlines. From the graphs we can see that near the tube walls more trapped boluses can be seen because there is some fluid resistance and at the centre fluid moves easily and free stream occurs at the centre of the tube. That is why tapped boluses cannot be seen at the centre of the tube and all the boluses can be seen only near the walls of the tube.

Evidently, the geometric and hydrodynamic parameters result in non-trivial modifications in the propulsion characteristics and these warrant further exploration in the future.

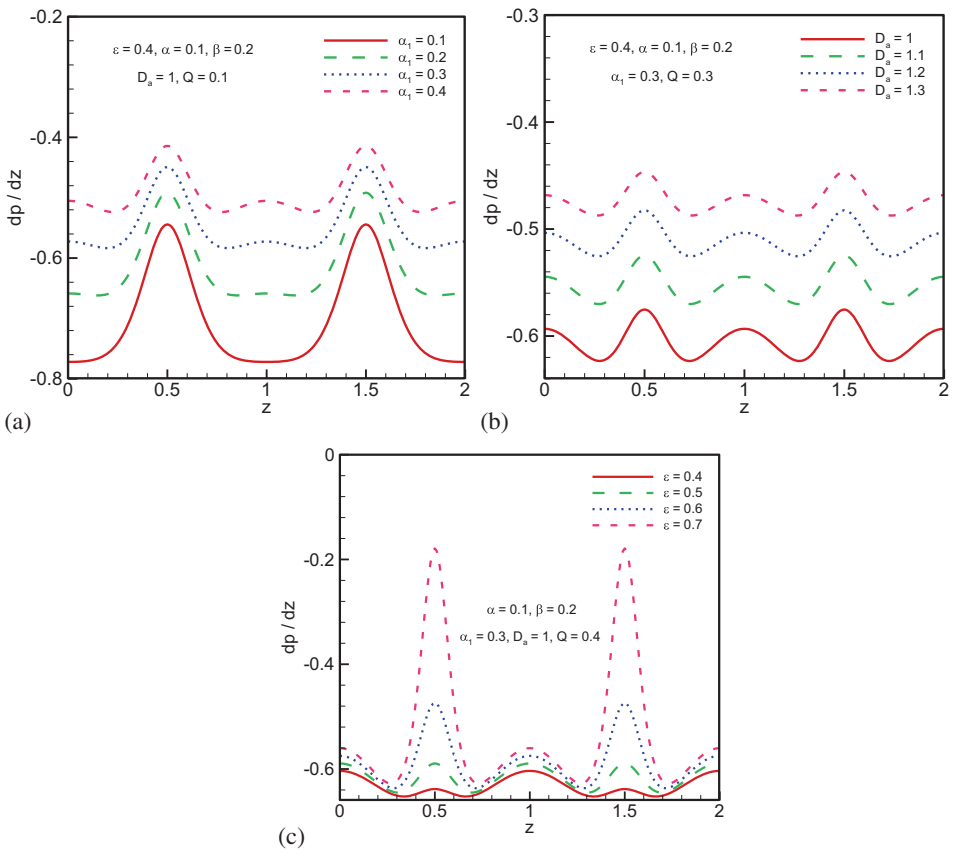


**Figure 4.** Pressure gradient vs. axial coordinate for (**a**) slip parameter $\alpha_1$, (b) Darcy number $D_a$ and (**c**) cilia length $\varepsilon$.

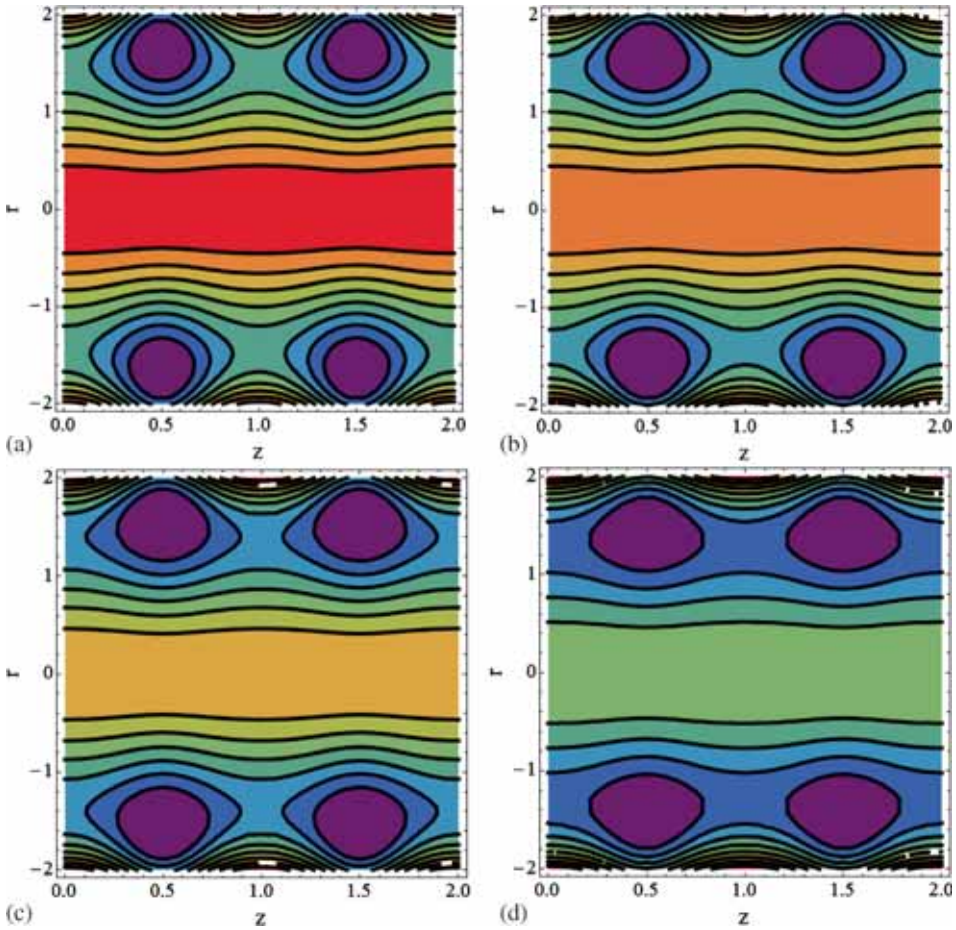


**Figure 5.** Streamlines for the velocity profile for slip parameters (**a**) 0.1, (**b**) 0.11, (**c**) 0.12 and (**d**) 0.15.

## 5. Concluding remarks

In this paper, a mathematical study has been conducted for creeping flow induced by a metachronal wave generated by beating of cilia tips in viscous propulsion through a porous medium-filled tube. The study has been motivated by further expounding biological propulsion mechanisms e.g. motion induced by cilia tips in urodynamics, breathing in the human respiratory system, sperm movement in reproductive system etc. Furthermore, the study is pertinent to biomimetic propulsion mechanisms exploiting surface treatments via artificial cilia. This work will further stimulate the much-needed laboratory investigations which would serve to garner vital experimental data. Although confined to viscous (Navier–Stokes) fluids and viscous-dominated porous media transport (Darcy model), some useful deductions can be made from the computations, namely:

1. Velocity is a decreasing function of slip parameter whereas it is an increasing function of Darcy number.
2. Greater flow rate increases axial velocity whereas the latter decreases with increasing axial coordinate.
3. Pressure rise reduces with increasing slip velocity and permeability (higher Darcy number) in the pumping region whereas the reverse trend is observed in the augmented pumping region.
4. Axial coordinate and Darcy number exert opposite effect on the pressure rise.
5. The size of trapped bolus in the streamline increases by increasing the magnitude of the slip parameter.

## Acknowledgement

Authors are thankful to the reviewer for useful suggestions to improve the manuscript.

## References


[1] T Y Wu, *Adv. Appl. Mech.* **38**, 291 (2001)

[2] T Y Wu, Reflections for resolution to some recent studies on fluid mechanics, in: *Advances in engineering mechanics – Reflections and outlooks* (World Scientific, Singapore, 2006)

[3] J Feng and S K Cho, *Micromachines* **5**, 97 (2014)

[4] Ye Wang, Yang Gao and Hans M Wyss, *Microfluid Nanofluid* **18**, 167 (2015)

[5] M A Sleigh, *The biology of cilia and flagella* (MacMillan, New York, USA, 1962)

[6] T J Lardner and W J Shack, *Bull. Math. Biophys.* **34**, 25 (1972)

[7] J R Blake, *J. Fluid Mech.* **55**, 1 (1972)

[8] T Y Wu, Fluid mechanics of ciliary propulsion, *Proc. Tenth Annual Meeting of the Society of Engineering Science* (Yale University, Connecticut, USA, 1973)

[9] C Brennen, *J. Fluid Mech.* **65**, 799 (1974)

[10] M A Sleigh and E Aiello, *Acta. Protozool.* **11**, 265 (1972)

[11] H Agarwal and A Uddin, *Indian J. Pure Appl. Math.* **15**, 1128 (1984)

[12] J R Blake, *J. Fluid Mech.* **46**, 199 (1971)

[13] C E Miller, An investigation of the movement of Newtonian liquids initiated and sustained by the oscillation of mechanical cilia, *Aspen Emphysema Conf.* (Aspen, Colorado, USA, 1967)

[14] C Barton and S Raynor, *Bull. Math. Biophys.* **29**, 419 (1967)

[15] D J Smith, E A Gaffney and J R Blake, *Bull. Math. Biol.* **69**, 289 (2007)

[16] A Dauptain, J Favier and A Battaro, *J. Fluid Struct.* **24**, 1156 (2008)

[17] S N Khaderi and P R Onck, *J. Fluid Mech.* **708**, 303 (2012)

[18] S N Khaderi, J M J den Toonder and P R Onck, *Biomicrofluidics* **6**, 014106 (2012)

[19] S N Khaderi, C B Craus, J Hussong, N Schorr, D J Belardi, J Westerweel, O Prucker, D J Ruhe, J M J den Toondere and P R Onck, *Lab Chip* **11**, 2002 (2011)

[20] G A Truskey, F Yuan and D F Katz, *Transport phenomena in biological systems* (Pearson, New Jersey, 2004)

[21] K Vafai, *Handbook of porous media* (Begell House, New York, USA, 2003)

[22] O Coussy, *Mechanics of porous continua* (Butterworths, USA, 1993)

[23] A R A Khaled and K Vafai, *Int. J. Heat Mass Transfer* **46**, 4989 (2003)

[24] P G Saffman, *Stud. Appl. Math.* **50**, 93 (1971)

[25] Y Miyamoto, M Hanano and T Iga, *J. Theor. Biol.* **102**, 585 (1983)

[26] B Jeffrey, H S Udaykumar and K S Schulze, *Am. J. Physiol. Gastrointest. Liver Physiol.* **285**, G907 (2003)

[27] E F Elshehawey, N T Eldabe, E M Elghazy and A Ebaid, *Appl. Math. Comput.* **182**, 140 (2006)

[28] A R Rao and M Mishra, *J. Non-Newtonian Fluid Mech.* **121**, 163 (2004)

[29] D Tripathi and O Anwar Bég, *J. Mech. Med. Biol.* **12(5)**, 1250088 (2012)

[30] D Tripathi and O Anwar Bég, *Transport Porous Med.* **95**, 337 (2012)

[31] R Ellahi, S U Rahman, S Nadeem and Noreen Sher Akbar, *J. Comput. Theor. Nanosci.* **11**, 1156 (2014)

[32] S Nadeem and H Sadaf, *Trans. Nanobiosci.* **14**, 447 (2015)

[33] Noreen Sher Akbar and Z H Khan, *Int. J. Biomath.* **8(2)**, 1550026 (2015)

[34] Noreen Sher Akbar, *Int. J. Biomath*. **8(2)**, 1550023 (2015)

[35] S Nadeem and H Sadaf, *Eur. Phys. J. – Plus (EPJ Plus)* **131**, 65 (2016)